AN EMPIRICALLY-CALIBRATED MODEL FOR INTERPRETING THE EVOLUTION OF GALAXIES DURING THE REIONIZATION ERA

Daniel P. Stark[1], Abraham Loeb[2], Richard S. Ellis[1]
Draft version May 20, 2008

ABSTRACT

We develop a simple star formation model whose goal is to interpret the emerging body of observational data on star-forming galaxies at $z \gtrsim 6$. The efficiency and duty cycle of the star formation activity within dark matter halos are determined by fitting the luminosity functions of Lyα emitter and Lyman-break galaxies at redshifts $z \simeq 5-6$. Our error budget takes proper account of cosmic variance arising from both the spatial clustering of galaxies and the commonly-used Poisson contribution. For a given survey geometry, we find a cross-over luminosity below which clustering provides the dominant contribution to this variance. Using our model parameters we predict the likely abundance of star forming galaxies at earlier epochs and compare these to the emerging data in the redshift interval $7 < z < 10$. We find that the abundance of luminous Lyman-break galaxies in the 500 Myr between $z \simeq 6$ and 10 can be naturally explained by the hierarchical assembly of dark matter haloes; there is only marginal evidence for strong physical evolution as has been claimed. In contrast, the first estimates of the abundance of less luminous star forming galaxies at $z = 9-10$ are higher than predicted and, if verified by further data, may suggest a top-heavy stellar mass function at these early epochs. Although these abundances remain uncertain because of the difficulty of spectroscopic confirmation, even a modest improvement in survey capability with present or upcoming facilities should yield great progress. In this context, we use our model to consider those observational techniques that hold the most promise and make predictions for specific surveys that are, or will soon be, underway. We conclude that narrowband Lyα emitter surveys should be efficient on searches at $z \simeq 7-8$; however, such conventional surveys are unlikely to detect sufficient galaxies at $z \simeq 10$ to provide useful constraints. For this reason, gravitational lensing offers the best prospect for probing the $z \simeq 10$ universe prior to JWST.

Subject headings: cosmology: theory — galaxies:formation — galaxies: high-redshift

1. INTRODUCTION

The recent discovery of star-forming galaxies at high redshifts, $z > 6$, represents an emerging frontier in our understanding of the early stages of galaxy formation. Such studies aim to determine the role that young galaxies may play in completing cosmic reionization, as well as to define more clearly how feedback and other poorly-understood processes shape the early distribution of galaxy luminosities and sizes from which later systems evolve (see reviews by Loeb 2006; Ellis 2007).

Considerable observational progress is being made through ambitious campaigns undertaken with the Hubble and Spitzer Space Telescopes and large ground-based telescopes. As a result, luminosity functions and stellar mass distributions are now available for various star-forming populations observed at z≃5–6. These include the continuum 'drop-outs' or Lyman break galaxies (LBGs,Bouwens et al. 2006; Yan et al. 2006; Eyles et al. 2006; Stark et al. 2006), and the Lyman-alpha emitters (LAEs, Santos et al. 2004; Malhotra & Rhoads 2004; Hu et al. 2004; Shimasaku et al. 2006; Kashikawa et al. 2006), located either spectroscopically or via narrow band imaging. Alongside these achievements, the first constraints are now emerging on the abundance of equivalent systems at $7 < z < 10$ (Richard et al. 2006; Willis & Courbin 2005; Bouwens & Illingworth 2006; Iye et al. 2006; Cuby et al. 2006; Stark et al. 2007).

Several questions arise as observers continue to make progress. First, what is the physical relationship between the Lyman Break Galaxy (LBG) and Lyman-alpha emitter (LAE) populations? This is important in interpreting the quite significant differences that have been observed between the properties of the two classes. Second, what redshift trends are expected for these populations? Some authors (e.g. Kashikawa et al. 2006; Bouwens & Illingworth 2006) have claimed strong evolution in the abundances with redshift. However, in the absence of any theoretical framework it is difficult to assess the significance of these claims. Finally, given the abundance of star forming galaxies at $z \simeq 5-6$, what is expected at $z \simeq 7-10$, the current observational target? And what is the optimum observational strategy for finding those sources which will be valuable in constraining the epoch of cosmic reionization and the properties of young galaxies?

The present paper is motivated by the need to answer these questions given the improving observational situation at $z \simeq 5-6$. As the time interval between $z=6$ and $z=10$ is short by cosmic standards ($\simeq 470$ Myr in the WMAP3 cosmology, Spergel et al. 2006), the growth of the halo mass function over this redshift range is well understood. Accordingly, it is practical to fit the $z \simeq 5-6$ observations in the context of a simple star-formation model, thereby deducing the likely differences between the LBG and LAE populations, and to then use such an empirically calibrated model to predict their likely abundances at $z \simeq 10$.

The model we adopt assumes all early star-forming galaxies observed during this relatively short period are primarily triggered into action by halo mergers. The key parameters governing their visibility are thus the efficiency of star formation and the duty cycle of its activity. An observed luminosity function at $z \simeq 5-6$ thus provides a joint constraint on the

[1] Department of Astrophysics, California Institute of Technology, MS 105-24, Pasadena, CA 91125; dps@astro.caltech.edu

[2] Astronomy Department, Harvard University, 60 Garden Street, Cambridge, Massachusetts 02138, USA

star formation efficiency (which determines the rate at which baryons are converted into stars) and the duty cycle of activity (which determines the fraction of halos occupied by visible galaxies). We consider such a simple model to be complementary and perhaps more intuitive than full *ab initio* numerical simulations which must also assume sub-grid presriptions for star formation (e.g Nagamine et al. 2005; Gnedin & Fan 2006). The goal is to infer the likely redshift trends in the context of emerging data and to use the model to evaluate the future observational prospects, particularly in the optimal design of surveys to locate sources at $z \simeq 10$ or so.

Several authors have already made good progress with such semi-analytic models. Le Delliou et al. (2005) and Dijkstra et al. (2006) have attempted to fit the luminosity distribution of LAEs. Dijkstra et al. argue that the evolution observed by Kashikawa et al. (2006) between $z = 5.7$ and $z=6.5$, claimed as arising from changes in the intergalactic medium, may be understood instead through simple growth in the halo mass function. Mao et al. (2006) have extended the method to contrast the properties of LAEs and LBGs; they find LBGs reside in a wide range of halo masses (10^{10} to $10^{12} M_\odot$), whereas LAEs reside within a narrower range ($\simeq 10^{11} M_\odot$). A key inference from their model is the short duty cycle of activity in the most luminous sources.

The present paper extends the earlier work by focusing not only on explaining the growing body of data at $z \simeq 5$–6. Here we will also include the emerging data at higher redshift to see how it agrees with our model predictions. A crucial ingredient in finding the model parameters that best fit the observational data is the error budget on that data. The commonly-used scatter due to Poisson fluctuations must be supplemented by the spatial clustering of galaxy halos within the volume of each survey. Here we will provide new error bars for existing data and show that the cosmic variance due to clustering dominates over Poisson fluctuations below a particular galaxy luminosity for a given survey geometry. This understanding can be used to optimize the flux sensitivity and strategies of future high-z surveys.

The plan of the paper is as follows. In §2 we introduce the basic ingredients of our model for star forming galaxies at high-redshifts. In §3 we calculate the error budget for observations of LBGs and LAEs at high redshift. The model is calibrated against existing data for LBGs and LAEs at $z \simeq 5$–6 in §4 and used to discuss the emerging data at earlier epochs in §5. In §6 we discuss the implications of our model for further observational campaigns with current and projected facilities. In §7, we summarize our conclusions.

Throughout the paper, we have assumed a flat universe and $(\Omega_m, \Omega_\Lambda)=(0.24, 0.76)$ following results in Spergel et al. (2006). All magnitudes are given in the AB system.

2. A PHYSICAL MODEL FOR HIGH REDSHIFT STAR FORMING GALAXIES

The rationale of this paper is to empirically-calibrate, using the data now available at $z \simeq 5$–6, the parameters of a simple model that describes the evolving luminosity function of star-forming galaxies (both LBGs and LAEs) over the quite short time interval corresponding to the redshift range $5 < z < 10$. Such a model can then be used to make predictions for the upcoming $z \simeq 7$-10 surveys.

The model assumes star formation at these early epochs is primarily triggered by the well-understood rate at which dark matter halos coalesce. We assume that the ratio of baryons to total mass in halos above some minimum mass

(Wyithe & Loeb 2006) follows the universal value Ω_b/Ω_m. Baryons are subsequently converted to stars with an efficiency given by $f_\star$. Following Loeb et al. (2005) and Wyithe & Loeb (2006), we define the star formation timescale, t_{LT}, as the product of the star formation duty cycle, ϵ_{DC}, and the cosmic time, $t_H \equiv 2/3H$ at that redshift. Using these ingredients, the star formation rate $\dot{M}_\star$ is related to halo mass M_{halo} as follows

$$\dot{M}_\star(M_{halo}) = \frac{f_\star \times (\Omega_b/\Omega_m) \times M_{halo}}{t_{LT}}. \quad (1)$$

For comparison to LBG samples, the star formation rate defined above is converted to the luminosity per unit frequency at 1500 Å following the prescription presented in Madau et al. (1998): $L_{1500} = 8.0 \times 10^{27} \dot{M}_\star/M_\odot \text{ yr}^{-1} \text{ erg s}^{-1} \text{Hz}^{-1}$. This conversion factor assumes a Salpeter initial mass function (IMF) of stars; if the IMF is more top-heavy than the Salpeter IMF, the far-ultraviolet luminosity will be greater for a given $\dot{M}_\star$.

Comparison to LAE samples requires converting the star formation rates derived above to a Lyα luminosity. We do this assuming that two-thirds of all recombining photons result in the emission of a Lyα photon (case B recombination). The ionizing photon production rate is calculated from the star formation rate for a given IMF and metallicity. We fix the metallicity at 1/20 solar and assume a Salpeter IMF which yields $N_\gamma = 4 \times 10^{53}$ ionizing photons per second per star formation rate in $M_\odot/\text{yr}$ (Schaerer 2003). An extreme top-heavy Population III IMF would produce 3×10^{54} ionizing photons (Bromm et al. 2001; Schaerer 2003), and we will consider such an IMF in later sections. Since the Lyα photons are assumed to be produced via recombinations, only the fraction of ionizing photons which do not escape into the intergalactic medium, $(1 - f_{ip})$, produce Lyα photons. Furthermore, only a fraction, $T_{Ly\alpha}$, of the emitted Lyα photons escape the galaxy and are transmitted through the intergalactic medium (IGM). With this prescription the Lyα luminosity is related to the halo mass as follows:

$$L_{Ly\alpha} = \frac{2}{3} h\nu_\alpha N_\gamma T_{Ly\alpha}(1 - f_{ip})\dot{M}_\star. \quad (2)$$

A substantial change in the IGM transmission parameter $T_{Ly\alpha}$ is expected to signal the end of reionization.

We also consider a more advanced model, incorporating the effects of supernova feedback on the luminosity function of star-forming galaxies. Since supernova feedback can significantly reduce the efficiency of star formation in low-luminosity galaxies, it is particularly important to consider when predicting the efficiency of future surveys for high-redshift galaxies aimed at detecting intrinsically fainter systems, rather than the luminous and rare objects that have been detected thus far, Following the scaling relations presented in Dekel & Woo (2003), we assume there is a critical halo mass at each redshift below which the star formation efficiency begins to decrease due to feedback. The star formation efficiency (which we now call $\eta(M)$) is a function of halo mass,

$$\eta(M_{halo}) = \begin{cases} f_\star \left(\frac{M_{halo}}{M_{halo,crit}}\right)^{2/3} & M_{halo} < M_{halo,crit} \\ f_\star & M_{halo} > M_{halo,crit} \end{cases} \quad (3)$$

where $M_{halo,crit}$ represents the critical value. At a given redshift, the critical halo mass can be related to a critical halo velocity. In the local universe, observations suggest a critical halo velocity of $\sim 100 \text{ km s}^{-1}$ (Dekel & Woo 2003); we adopt this for our high-redshift models, assuming that the physics of

supernova feedback depends only on the depth of the gravitational potential well of the halos.

Finally, in §6 we also consider the expected evolution of galaxy sizes. This is particularly important for gauging the efficiency of future surveys utilizing adaptive optics in detecting galaxies at $z \gtrsim 7-20$. If a galaxy is resolved in a particular observation, the signal-to-noise ratio for the detection increases as the size of galaxy decreases since a smaller aperture (with less noise) is required to encircle its flux. Next-generation adaptive optics systems on thirty-meter class ground-based telescopes will offer a resolution of >9 milliarcseconds at $1.1 \mu m$, corresponding to $\simeq 50$ pc at $z \simeq 7$. With such exquisite angular resolution, the size of early galaxies is likely to be a limiting factor in their detection.

We assume that the extent of the stellar region of a galaxy at a particular epoch is a constant fraction of the size of the host dark matter halo. The virial radius of a halo is given by

$$r_{vir} = \left[\frac{G M_{vir}}{100 H^2(z)} \right]^{1/3} \qquad (4)$$

where M_{vir} is the halo virial mass and $H(z) = H_0 [\Omega_{\Lambda,0} + (1 - \Omega_{\Lambda,0} - \Omega_0)(1+z)^2 + \Omega_0(1+z)^3]^{1/2}$ is the Hubble canstant at redshift z. At very high redshift, the halo virial radius scales as $(1+z)^{-1}$ for fixed halo mass. Following the parameterization presented in Barkana & Loeb (2000), a typical galaxy brighter than 1 nJy between $5 \lesssim z \lesssim 10$ will have a disk radius of $0\rlap{.}''1$-$0\rlap{.}''2$, with the range depending on the efficiency with which baryons are converted to stars.

Observations lend support to this simple scaling of disk radius with redshift: $z \simeq 2-6$ dropouts in the Hubble Ultra Deep Field (UDF) and Hubble Ultra Deep Field Parallels (UDF-P) are best fit by a $(1+z)^{-1}$ power law for a fixed luminosity Bouwens et al. (2004). The mean half-light radius of 0.3-1.0 $L_{\star,z=3}$ LBGs at $z \simeq 6$ is 0.8 kpc, corresponding to $0\rlap{.}''1$ at $z \simeq 6$, consistent with the model presented in Barkana & Loeb (2000). To make predictions for future observations in §6, we thus assume the mean size of galaxies of similar luminosity scales as $0\rlap{.}''1(1+z/7)^{-1}$.

3. THE EFFECT OF VARIANCE IN DEEP SURVEYS

Interpreting and planning observations of galaxies in the reionization era requires an accurate understanding of uncertainties arising from both Poisson errors and fluctuations in the large-scale distribution of galaxies. For example, one of the main motivations for galaxy surveys at $z \simeq 7$–10 is the question of whether the imprint of reionization can be seen in the evolution of LAEs (Malhotra & Rhoads 2006; Dijkstra et al. 2006) or dwarf galaxies (Barkana & Loeb 2006; Babich & Loeb 2006). However, to answer these questions, it is important to ensure that the variance is less than the claimed evolution. In this section, we develop the formalism necessary to compute the variance for narrowband, dropout, and spectroscopic lensing surveys, and we then apply this formalism to recent surveys. An analysis of clustering variance was presented in Somerville et al. (2004). We improve upon two simplifications made in that work, both of which we discuss below.

The variance due to Poisson errors is given by $\mathcal{N}_i$, where $\mathcal{N}_i$ is the number of galaxies in luminosity bin i. To compute this we determine the number density of galaxies (either LBGs or LAEs) as a function of luminosity using the best-fitting models described in §4, from which we can determine the predicted counts for a given survey volume. When characterizing the variance at redshifts where data is sparse ($z \gtrsim 7$),

we assume no evolution in the model parameters from $z \simeq 6$. This method clearly has its limitations when probing new parameter space (e.g. low luminosities or high redshifts) where the abundance of galaxies is not well-known. However, given the lack of data, we consider it to be the simplest approach.

The clustering of galaxies in overdense regions causes fluctuations in galaxy counts, often referred to as cosmic variance. Determining this variance requires knowledge of the mass of the dark matter haloes that host the observed galaxies. If the correlation function of the galaxy population is known the clustering variance can be predicted for a given field of view. Moreover, if the data set is sufficiently large, the correlation function can be derived separately for bright and faint galaxies, thereby showing how the dark matter halo mass (and hence the clustering variance) varies with galaxy luminosity. A detailed spatial correlation function analysis is very challenging for current observations at $z \gtrsim 6$; hence an alternative method is needed for deriving the clustering variance.

Using the LBG and LAE model described in §2, the halo mass can be determined as a function of galaxy luminosity. The clustering variance can then be calculated for a given halo mass by taking the product of the variance of dark matter in the survey volume and the bias factor associated with halos of a given mass M. With this method, we compute the clustering variance as a function of galaxy luminosity for narrowband, dropout, and spectroscopic lensing surveys, taking into consideration the survey geometry specific to each survey.

First, we compute the variance of dark matter in a given smoothing window as follows:

$$\sigma^2(r) = \int P(k) \tilde{W}^2(\mathbf{k}) d^3\mathbf{k} \qquad (5)$$

where $P(k)$ is the power spectrum of density fluctuations extrapolated to z=0 as a function of wavenumber k and $\tilde{W}^2(\mathbf{k})$ is the Fourier transform of the window function in real space. The form of window function depends on the survey geometry; in the following subsections, we detail the window functions adopted in our analysis. Non-linear corrections to the power spectrum and probability distribution become important if the variance is larger than unity. In computing the variance, we adopt the non-linear power spectra using the halo model fitting functions presented in Smith et al. (2003). While fluctuations are in the linear regime, their probability distribution is Gaussian. However, in the non-linear regime, the probability distribution function appears to be well-described by a log-normal distribution (Kayo et al. 2001). Confidence intervals are thus determined via the geometric mean and standard deviation; the one-sigma upper and lower bound are given by $\exp(\mu+\sigma)$ and $\exp(\mu-\sigma)$, respectively, where μ and σ are the mean and standard deviation of the logarithm of a given density fluction, $\ln \delta$. If the standard deviation of the log-normal distribution is much less than one, $\sigma_{LN} \ll 1$, the probaility distribution function reduces to Gaussian with confidence intervals given by $\mu \pm \sigma$.

The clustering variance in the distribution of *galaxies* is then estimated by multiplying the variance in dark matter by the halo bias, which is defined as the ratio of the rms fluctuations of haloes to that of dark matter. We adopt the halo bias formula derived for the ellipsoidal collapse model by Sheth et al. (2001).

A key assumption in the clustering variance formalism described above is that there is not more than one galaxy per halo. More complex occupation numbers are possible, but since cooling is efficient at such high redshifts, the simplest
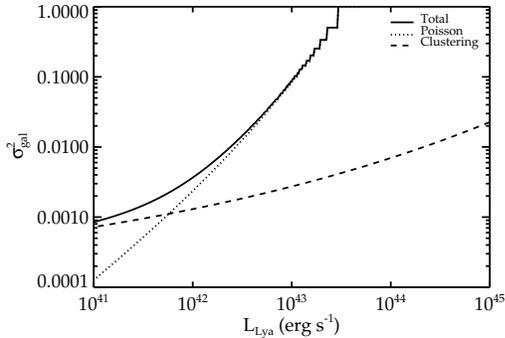
FIG. 1.— Variance in a narrowband Lyα survey. The total variance (solid line) is the sum of the variance from Poisson noise (dotted line) and clustering fluctuations (dashed line). The survey specifications adopted in the left panel are equivalent to Subaru survey for Lyα emitters at $z = 5.7$ (Shimasaku et al. 2006). The clustering fluctuations in such a narrowband survey are very small (less than 6%) in the luminosity range over which Lya emitters are detectable.

case is that with one galaxy per halo.

Now we introduce two key differences between our approach and that of Somerville et al. (2004). First, the survey geometry was assumed to be spherical in Somerville et al. (2004). However, different survey geometries may have substantially different power spectra (Kaiser & Peacock 1991). This is a particular concern for strong lensing surveys that utilize longslit spectroscopy (Santos et al. 2004; Stark et al. 2007). Second, the observed number density of the population was assumed to be equivalent to the number density of the underlying dark matter halos (Somerville et al. 2004). This assumption could be in error if the star formation duty cycle, ϵ_{DC}, is significantly smaller than unity. In this case, the observed number density of galaxies would be less than that of their host dark matter haloes by a factor of ϵ_{DC}. Depending on the slope of the mass function, this would overestimate or underestimate the cosmic variance.

In the following subsections, we apply the formalism described above to recent surveys for LBGs and LAEs. For each survey, we compute the typical amplitude of clustering and Poisson fluctuations in the relevant observational regime. In addition, we determine the cross-over luminosity, L_c, defined as the luminosity above which the Poisson error dominates that from clustering fluctuations.

3.1. *Variance in Narrowband Surveys*

The geometry of a narrowband LAE can be approximated as a rectangular parallelepiped with a comoving volume of $a_x a_y a_z$, where a_x and a_y are the comoving distances corresponding to the areal field of view of the survey and a_z is the comoving line-of-sight distance of the survey. The window function in k-space is simply the Fourier transform of a rectangular top-hat with dimensions corresponding to the survey geometry:

$$\tilde{W}(k_x, k_y, k_z) = \frac{\sin(k_x a_x/2)}{(k_x a_x/2)} \frac{\sin(k_y a_y/2)}{(k_y a_y/2)} \frac{\sin(k_z a_z/2)}{(k_z a_z/2)}. \quad (6)$$

Using the window function defined above, we evaluate the expected variance in narrowband surveys for LAEs at $z \simeq 6$. We focus our analysis on the narrowband surveys conducted at $z = 5.7$ and $z = 6.5$ in the Subaru Deep Field (SDF). Using the wide-format, Suprime-Cam (Miyazaki et al. 2002) on the Subaru Telescope, the observations sample an area of $34' \times 27'$ in the NB816 and NB921 narrowband filters. The central

wavelength and FWHM of the NB816 and NB921 filters are (8150 Å, 120 Å) and (9196 Å, 132 Å) respectively.

In Figure 1, we plot the variance in the $z = 5.7$ narrowband survey of the SDF. The Lyα luminosities probed in the Subaru survey range from $\simeq 10^{42} - 10^{43}$ erg s^{-1}. The clustering variance is less than $\simeq 0.01$ over this luminosity range, resulting in less than 10% uncertainty in the observed counts. Poisson errors dominate the clustering errors for sources brighter than the cross-over luminosity of $10^{41.7}$ erg s^{-1}.

3.2. *Variance in Lyman-break Surveys*

We focus our dropout survey analysis on the two $16' \times 10'$ Great Observatories Origins Deep Surveys (GOODS) of the Hubble Deep Field North (HDF-N) and Chandra Deep Field South (CDF-S) and the $3.4' \times 3.4'$ Hubble Ultra Deep Field (UDF). The redshift distribution of dropouts depends on the filters and color-cuts used in their selection. While the typical color-selection criteria for $i-drops$ select galaxies between $z = 5.5$ and $z = 7.0$ (Bunker et al. 2004), the effective distance sampled along the line-of-sight is less than the total comoving radial distance in this redshift interval because of incompleteness arising from objects being scattered faintward of the magnitude limit or out of the color-selection window. This incompleteness has been quantified in both GOODS and the UDF (Bunker et al. 2004; Bouwens & Illingworth 2006), allowing an effective volume to be derived for each survey. We approximate the geometry of the LBG survey as a rectangular parallelepiped with a characteristic line-of-sight distance equal to the ratio of the effective volume and the survey area and with dimensions in the plane of sky corresponding to the field-of-view of the survey.

The variance of the GOODS and UDF surveys for $z \simeq 6$ LBGs is presented in Figure 2. The GOODS survey is sensitive to sources brighter than 5×10^{28} erg s^{-1} Hz^{-1} (corresponding to a 10σ limit of z'_{AB}=26.5). At this limit, the clustering variance is only 0.005, and the total variance is dominated by the Poisson term. The clustering fluctuations are significantly lower than those estimated in Somerville et al. (2004), due largely to the more realistic model of a Gaussian redshift distribution of dropout sources. In the UDF, both the clustering and Poisson error are larger due to the smaller survey volume. The 8σ limiting far UV luminosity in the UDF is 8×10^{27} erg s^{-1} Hz^{-1}. The total variance at this limit is again dominated by clustering fluctuations, which contribute an uncertainty of $\sim$19% to the observed densities.

3.3. *Variance in Lensed Longslit Spectroscopic Surveys*

The geometry of a longslit spectroscopic survey can be approximated as a rectangular parallelepiped. However, in the case of a strong lensing longslit spectroscopic survey, the geometry is potentially slightly more complex. For a lensing survey, the slit geometry only corresponds to the *image* plane; however, we are interested in the geometry of the survey in the *source* plane, which can be calculated accurately via ray tracing if a reliable mass model is available. While the source plane geometry depends on the location of the longslit relative to the critical line, for typical clusters studied in Stark et al. (2007) it is well-approximated by a rectangular-parallelepiped (J. Richard 2006, private communication). The source plane area is reduced by a factor of the lensing magnification, $\mathcal{M}$; further, the magnification is not isotropic and is strongest perpendicular to the cluster critical line. Hence, assuming the longslit is oriented along the cluster critical line,
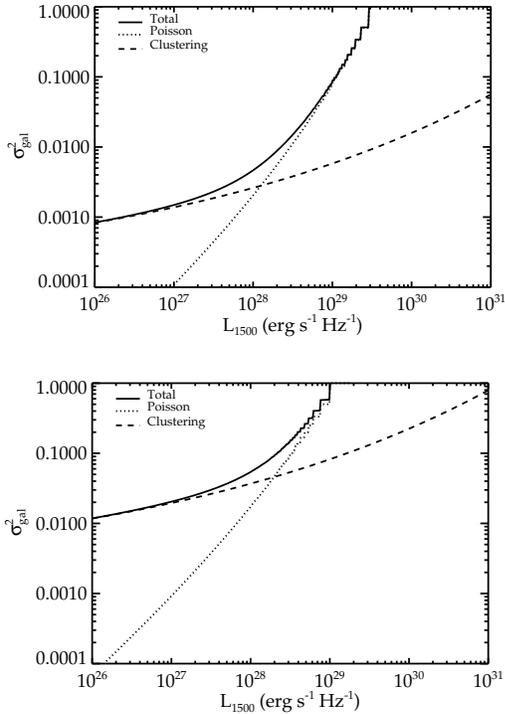
FIG. 2.— Variance in dropout LBG survey. The total variance (solid line) is the sum of the variance from Poisson noise (dotted line) and clustering fluctuations (dashed line). In the case of a survey such as the HST-GOODS observations of the CDF-S and HDF-N (limiting luminosity of $5 \times 10^{28} \mathrm{ergs}^{-1}\mathrm{Hz}^{-1}$), the clustering fluctuations of $z \simeq 6$ LBGs are greater than $\simeq 7\%$ (top panel). In the Hubble Ultra Deep field (limiting luminosity of $8 \times 10^{27} \mathrm{ergs}^{-1}\mathrm{Hz}^{-1}$), clustering fluctuations result in a slightly higher uncertainty of $\gtrsim 19\%$ (bottom panel).

the slit-width is compressed more than the slit-length. For the computations that follow, we assume the source plane slit width, a_x, is related to the image plane slit width, a'_x by $a_x = a'_x/\sqrt{2\mathcal{M}}$, and likewise, the source plane slit width is given by $a_y = a'_y \sqrt{2/\mathcal{M}}$, in agreement with typical slit positions from Stark et al. (2007).

As with the narrowband survey, the appropriate window function is a three-dimentional rectangular top-hat in real space, which in k-space corresponds to the product of three sinc functions (see Equation 6).

A typical near-infrared spectrometer has dimensions of $1\rlap{.}''$ $\times 40\rlap{.}''$ (Stark et al. 2007), which at $z \simeq 9$ corresponds to a comoving distance of 11 kpc$\times$900 kpc, assuming a median magnification factor of $\mathcal{M}=10$. In each cluster, an area is mapped out perpendicular to the critical line; assuming five slit positions are observed, this results in a total survey area of 9600 kpc^2. If observations are conducted in the J-band between $z = 8.5$ and $z = 10.4$, the comoving line-of-sight distance spanned is 479 Mpc. The clustering variance is decreased by observing along many independent sightlines; we adopt a thirty cluster survey for our calculations.

The clustering fluctuations are significantly larger in the spectroscopic lensing survey than in either the narrowband or dropout surveys due to the much smaller survey volumes sampled. The development of larger and more sensitive near-infrared spectrometers is necessary to decrease the clustering variance in such surveys.

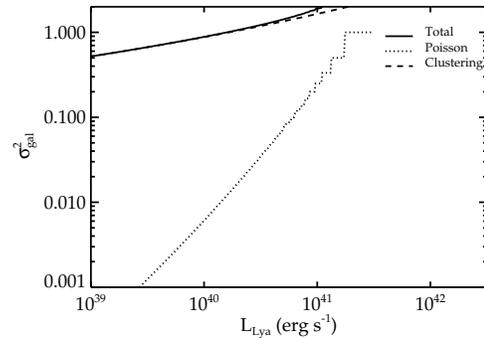## 4. MODEL CALIBRATION USING $Z \simeq 5-6$ OBSERVATIONS

FIG. 3.— Variance in a $z = 10$ lensed longslit spectroscopic survey. The total variance (solid line) is the sum of the variance from Poisson noise (dotted line) and clustering fluctuations (dashed line). The uncertainty from clustering fluctuations is significantly greater than the Poisson noise for all luminosities and is nearly 100% for sources with Lyα luminosities of 10^{40}-10^{41} and erg s^{-1}.

We are now in a position to use our model and our improved understanding of the effects of cosmic variance to constrain its parameters using observations of the luminosity functions at $z \simeq 5$–6. By doing this independently for LBGs and LAEs we will hopefully gain valuable insight into the physical differences between these two star-forming populations.

4.1. *Lyman-Break Galaxies*

Lyman-break galaxies are perhaps more straightforward to model than Lyα emitters because of the complex resonant interaction of Lyα photons with neutral hydrogen which occurs in the latter population. In our model of LBGs described in §2, there are two free-parameters: the star formation efficiency $f_\star$ and the duty cycle ϵ_{DC}. First we determine these parameters by reproducing the observations at $z \simeq 6$. We later use this model to consider whether the emerging data at $z \simeq 7-10$ requires any adjustment. Significant evolution in the model parameters between the two redshifts might signify some external phenomenon, such as the reionization of the intergalactic neutral hydrogen. Alternatively it could cast doubt on the reliability of the observations.

We compute a grid of LBG luminosity functions by varying $f_\star$ and ϵ_{DC}. The comoving number density of galaxies predicted by the models, n_{mod}, is compared to the observed value, n_{obs}, in each of the N luminosity bins, and a likelihood of a given set of parameters is defined such that $\mathcal{L}(f_\star, \epsilon_{DC}) = \exp[-0.5\chi^2]$, where $\chi^2 = \Sigma_{i=1}^{N}(n_{obs,i} - n_{mod,i})$.

We first apply our model to the observed abundance of LBGs at $z \simeq 6$, as compiled by Bouwens et al. (2006). In Figure 4, we show the likelihood contours at 64% and 26% of the peak likelihood (corresponding to 1- and 2-σ for a Gaussian distribution). The maximum likelihood and 1-σ confidence intervals are $(f_\star, \epsilon_{DC}) = [0.1^{+0.05}_{-0.04}, 0.08^{+0.2}_{-0.06}]$, in reasonable agreement with a similar fit to these observations in Wyithe & Loeb (2006). When supernova feedback is allowed to decrease the star formation efficiency in low-mass halos (see §2 for details), the best-fit parameters change slightly: $(f_\star, \epsilon_{DC}) = [0.25^{+0.03}_{-0.03}, 0.4^{+0.10}_{-0.15}]$. The strong degeneracy between the duty cycle and the star formation efficiency arises because an increase in the star formation efficiency requires a longer star formation timescale (and hence larger star formation duty cycle) to produce the same far-UV luminosity for a given halo mass.

Although there is some degeneracy between the best-fitting star formation efficiency and duty cycle at $z \simeq 6$, the range
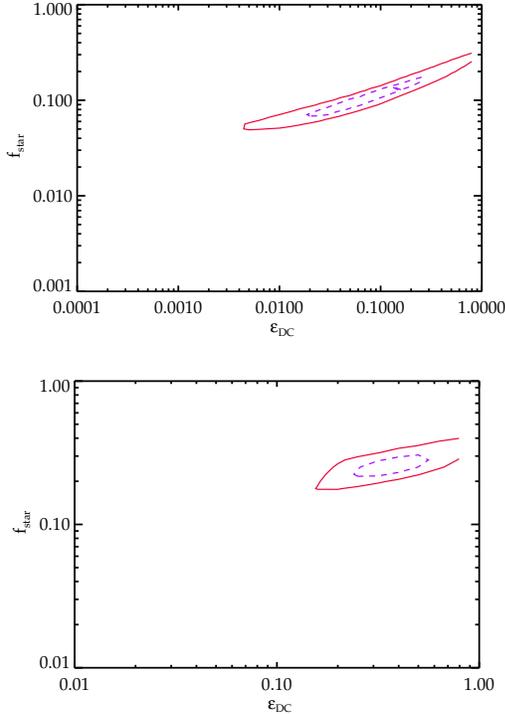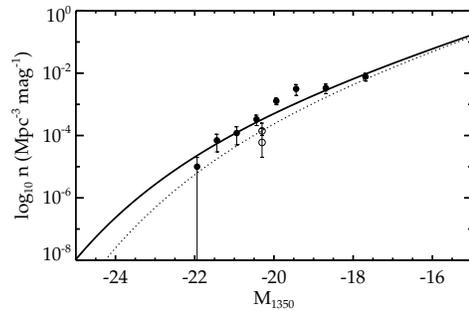
FIG. 5.— The LBG luminosity function at z=6 (solid line) and z=7.6 (dotted line) obtained using the model parameters that maximize the likelihood at z=6. The solid and open circles correspond to observed LBG abundances at z=6 (Bouwens et al. 2006) and z=7.6 (Bouwens & Illingworth 2006). The two datapoints at z=7.6 correspond to more and less conservative selections of z-drops in Bouwens & Illingworth (2006). While there is not yet much data at z=7.6, the existing data at these two redshifts can be fit without any evolution in the fit parameters $f_\star$ and ϵ_{DC}.

FIG. 4.— *Top:* Confidence intervals on star formation efficiency $f_\star$ and duty cycle ϵ_{DC} in a simple theoretical model for the observed abundances of LBGs at z=6. The likelihood contours are 64% and 26% of the peak likelihood. *Bottom:* Same as above except with supernova feedback included in model.

of values can be physically understood. A duty cycle of 8% at $z \simeq 6$ corresponds to a star formation lifetime of 80 Myr which is roughly the same as the dynamical time of virialized halos (or the duration of equal-mass mergers) at that redshift. Our simple model thus suggests that at $z \simeq 6$, star formation is proceeding on the same timescale it takes virialized baryons to settle to the center of the galaxy. A star formation efficiency of $\sim 10\%$ is reassuringly similar to the ratio between the global mass density in stars and baryons in the present-day Universe (Fukugita et al. 1998).

An independent check on the inferred duty cycle could conceivably be obtained if the spectral energy distribution were known for a large sample of $z \simeq 5$–6 LBGs. Fitting these with a grid of population synthesis models Bruzual & Charlot (2003) allows, in principle, the estimation of the stellar mass, dust extinction, and luminosity-weighted age of representative galaxies. Unfortunately, the ages inferred via this technique have large systematic uncertainties due to the inability of the population synthesis models to constrain the past star formation history (Eyles et al. 2006; Shapley et al. 2005). Taking the star formation histories that minimize the χ^2 fit to the SEDs of LBGs at $z \simeq 6$, Eyles et al. (2006) find a median age of 500 Myr for those objects detected in the rest-frame optical with Spitzer (and hence the most massive objects). A stacking analysis of the least massive LBGs in their survey indicates that these objects have ages of $\simeq 60$ Myr. Recalling that the duty cycle is equal to the star formation timescale divided by the cosmic time, these inferences suggest that the duty cycle lies in the range 6-50% and perhaps increases with the mass of the galaxy.

A further check is provided by limited data on the clustering of LBGs. The halo masses probed in the Bouwens et al. (2006) compilation in the GOODS and UDF surveys are 5 ×

$10^9 M_\odot$–$2 \times 10^{11} M_\odot$ according to the simple model we have adopted. These values are consistent with clustering analysis of $z \simeq 6$ LBGs in GOODS, which suggest that the hosting dark matter haloes are $\sim 10^{11} M_\odot$ (Overzier et al. 2006). Reionization would be accompanied by a dramatic increase in the cosmological Jeans mass and and therefore in the minimum galaxy mass (Wyithe & Loeb 2006). A direct detection of this effect requires finding galaxies in dark matter haloes over an order of magnitude less massive than those probed in current surveys (Barkana & Loeb 2006).

One important implication of our best-fit duty cycle is that $\simeq$90% of dark matter halos of a given mass are not traced by LBGs. The "missing" dark matter halos may have gone through bursts of star formation at earlier times and may be currently quiescent. However, this does not mean that 90% of the stellar mass is missing from observations at $z \simeq 6$. Rather, the gas in the "missing" dark matter halos may not have cooled sufficiently to be forming stars rapidly enough to be selected as LBGs and thus may not be significant repositories of stellar mass. The first option suggests that there may have been a significant amount of star formation at earlier times. This is evidenced by observations of LBGs at $z \simeq 6$ with stellar masses as great as a few $\times 10^{10} M_\odot$ and ages of 200-700 Myr (Eyles et al. 2005, 2006). Given the current observed star formation rate of these galaxies, the past star formation rate had to have been higher at earlier times. The 10% duty cycle inferred from the luminosity function of the LBGs provides additional, independent evidence that the purported deficit of ionizing photons compared to that required for reionization (Bunker et al. 2004; Bouwens et al. 2006) at $z \simeq 6$ could be accounted for by earlier star formation.

4.2. *Lyα emitters*

We now use a procedure similar to that described for the LBGs to model the LAEs. The key difference is that we must also consider the fraction of Lyα photons that escape from the galaxy and IGM, T_α. We generate a grid of models at $z = 5.7$ and $z = 6.5$ with the duty cycle, ϵ_{DC} ranging from 10^{-3} and 1 and the product of the star formation efficiency and Lyα escape fraction, $f_\star T_\alpha$ spanning between 10^{-3} and 1. Each model is compared to the observed abundances, and the likelihood is then determined for each model in an identical fashion to that discussed for the LBGs. We first perform this procedure
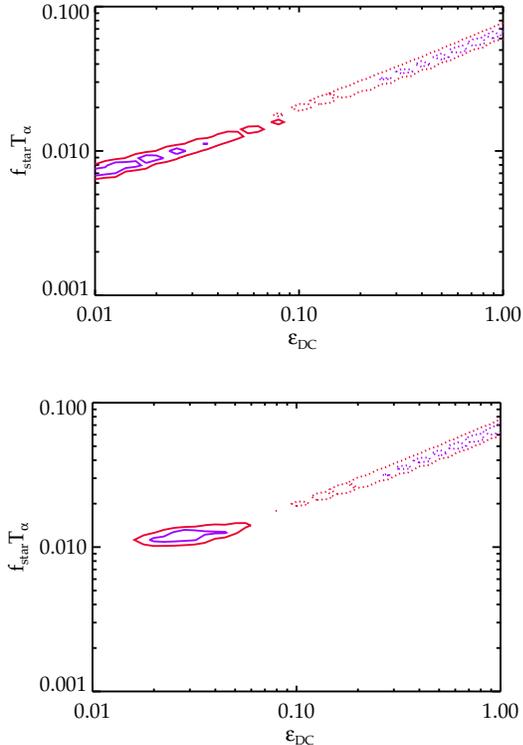
FIG. 6.— *Top:* Confidence intervals on free parameters in analytic fit of observed LAE abundances at z=5.7 (solid lines) and z=6.5 (dotted lines). The likelihood contours are 64% and 26% of the peak likelihood. The parameters that maximize the likelihood are $(\epsilon_{DC}, f_{star}T_\alpha)$=(0.02,0.009) at z=5.7 and $(\epsilon_{DC}, f_{star}T_\alpha)$=(0.9,0.06) at z=6.5. *Bottom:* Same as Figure 6a with the addition of a simple prescription for supernova feedback.

FIG. 7.— *Top:* The Lyα luminosity function at z=5.7 (dotted line) and z=6.5 (solid line) obtained using the model parameters that maximize the likelihood. Open and solid circles are observed abundances at $z = 5.7$ from Shimasaku et al. (2006) and at $z = 6.5$ from Kashikawa et al. (2006). *Bottom:* Same as above but for best-fitting parameters to model that now includes a simple prescription for supernova feedback.

for our simple model and then examine it in the context of a model including supernova feedback.

Likelihood contours are presented in the top panel of Figure 6 for $z = 5.7$ (solid contours) and $z = 6.6$ (dotted contours). As with the fit to the LBGs, there exists a strong degeneracy between ϵ_{DC} and $f_\star T_\alpha$. The best-fitting parameters (with associated one-sigma errors) are $(\epsilon_{DC}, f_\star T_\alpha) = (0.02^{+0.02}_{-0.01}, 0.009^{+0.001}_{-0.002})$ at $z = 5.7$ and $(\epsilon_{DC}, f_\star T_\alpha) = (0.9^{+0.1}_{-0.6}, 0.06^{+0.01}_{-0.03})$ at $z = 6.5$. The $z = 5.7$ data are significantly better fit (factor of 4 greater maximum likelihood at $z = 5.7$) by the advanced model including supernova feedback (bottom panel of Figure 6). The best-fitting parameters at $z = 6.5$ remain unchanged, while those at $z = 5.7$ change marginally: $(\epsilon_{DC}, f_\star T_\alpha) = (0.03^{+0.01}_{-0.01}, 0.01^{+0.001}_{-0.001})$.

The best-fitting luminosity functions are plotted over the observed abundances in the top panel of Figure 7 (simple model) and in the bottom panel of Figure 7 (advanced model with supernova feedback). The error bars in these plots include both Poisson and clustering variance. Examining the confidence intervals and luminosity functions, it seems that the data suggest some evolution in the best-fitting model parameters between z=5.7 and z=6.5. It is unlikely that the evolution is associated with a change in the neutral fraction of the IGM because the parameter that is proportional to the transmission of Lyα photons, $f_\star T_{Ly\alpha}$, increases between z=5.7 and z=6.5, contrary to what would be expected if the neutral fraction increased. Taken at face value, the evolution in the model parameters suggests that the star formation efficiency and lifetime in LAEs increases between $z = 5.7$ and $z = 6.5$. However, uncertainties in the observations make these con-
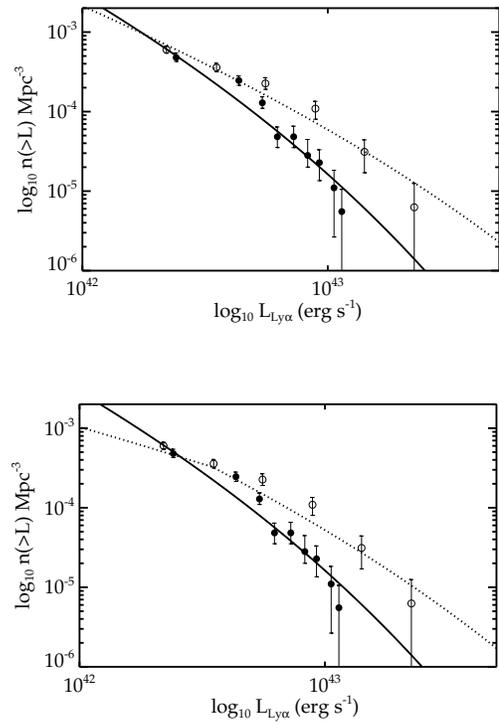
clusions tentative. The LAE luminosity function adopted in this paper is based on a photometric sample of objects selected with a narrowband filter. While many of the most luminous photometrically-selected objects have been confirmed spectroscopically, at lower luminosities the completeness is still low. It is possible that there is significant contamination from low-redshift line emitters, and hence that the densities at these low luminosities are overestimated. Indeed, if the $z = 6.5$ model parameters are held fixed at the best-fit $z = 5.7$ values, the observed low-luminosity densities are significantly greater than the model predictions (Figure 8). If the error bars at low luminosities are enlarged to reflect this uncertainty, then the model parameters are consistent with no evolution between $z = 5.7$ and $z = 6.5$ except in the underlying halos (Dijkstra et al. 2006). Additional spectroscopic observations of the lowest luminosity LAEs are clearly necessary to resolve whether the physical parameters of LAEs evolve between z=5.7 and z=6.5.

We now examine the consistency of our best-fit model parameters in the context of additional observations of $z \gtrsim 5$ LAEs. Recently, observations have shown that luminous LAEs at $z \simeq 5$ have relatively low stellar masses. LAEs at $z \simeq 5$ with $L_{Lya} \simeq 10^{42} - 10^{43} ergs^{-1}$ have $M_{stellar} \simeq 10^6 - 10^8 M_\odot$ (Pirzkal et al. 2006). Assuming the ratio of baryons to total mass follows the universal value Ω_b/Ω_m and a star formation efficiency of $\simeq 10\%$, the observed stellar masses suggest halo masses of $6 \times 10^7 - 6 \times 10^9 M_\odot$. According to our best-fit models, the halo masses probed by the Subaru observations are signficantly greater: at $z = 5.7$ halo masses range from 10^{10} to $10^{11} M_\odot$, while at $z = 6.5$, the halo masses range be-

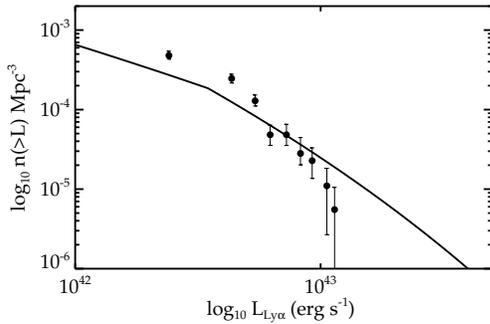Fig. 8.— The Lyα luminosity function at z=6.5 obtained using the model parameters that maximize the likelihood at z=5.7 (allowing for supernove feedback). Solid circles are observed abundances at $z = 6.5$ from Kashikawa et al. (2006). Error bars on datapoints include contribution from Poisson and clustering variance. The model underpredicts the data at low luminosities. This could potentially be explained by low-redshift line emitters contaminating the low luminosity datapoints.

tween 5×10^{10} and 5×10^{11} M$_\odot$.

Given the low stellar masses observed for these objects, it seems that one of our assumptions must be incorrect. Under our simple model, the stellar mass is given by M$_{stellar}$ = f$_\star$[Ω_b/Ω_m]M$_{halo}$; in order to decrease the stellar mass for a given halo mass, the star formation efficiency must be lower than the 10% value we have assumed above. However, the star formation efficiency must also satisfy the relation between Lyα luminosity and halo mass (equation 2) which is constrained via the observed abundance of LAEs as a function of luminosity. Hence, if the star formation efficiency decreases, either the Lyα transmission factor or the ionizing photon rate must increase to satisfy equation 2. The latter could occur if the IMF of stars was more top-heavy than the standard Salpeter form. While a top-heavy IMF would reduce the stellar mass predicted by our model, it would also decrease the observationally inferred LAE stellar masses. These masses have been inferred via population synthesis models assuming a Salpeter IMF. Top-heavy IMFs have a lower rest-frame optical stellar mass-to-light ratios then the Salpeter IMF does; hence, for a given luminosity, the inferred mass in stars is lower than for a Salpeter IMF. Therefore, the stellar masses inferred from observations remain at odds with those predicted from our models. Alternatively, if the Lyα transmission fraction, T$_{Ly\alpha}$, is enhanced to account for the lower star formation efficiency, the models achieve much better agreement with the observations. At z = 5.7, our best-fitting models have f$_\star$T$_{Ly\alpha}$ ≃ 0.01. If the Lyα transmission factor is near unity, then the star formation efficiency is roughly 1%. In this scenario, the stellar masses predicted by the models are ≃ $10^7 - 10^8$ M$_\odot$ at z = 5.7, in much closer agreement with the observations.

The low star formation efficiency and large Lyα transmission factor of LAEs can be understood physically. In addition to showing that the brightest LAEs have low stellar masses, observations have also shown that the most luminous LAEs are a young population with ages of a few ×10^6 years (Pirzkal et al. 2006; Finkelstein et al. 2006), comparable to the lifetime of massive stars before they may explode as supernovae. Hence, these galaxies are observed at such a young stage that they have not had sufficient time to convert more than roughly 1% of their baryons to stars. Moreover, they likely have not had enough time to produce a sig-

nificant amount of dust. This conjecture is corroborated by population synthesis modeling of the observed SEDs of $z \simeq 5$ LAEs (Gawiser et al. 2006). Without dust to absorb the resonantly scattered Lyα photons, the fraction of Lyα photons escaping the galaxy may increase substantially, explaining the very large Lyα transmission factor needed to fit the observed stellar masses. However, the Lyα transmission factor is also dependent on intergalactic absorption. The typical flux decrement encountered by Lyα photons in the intergalactic medium (Fan et al. 2006) may be substantially reduced in the vicinity of LAEs if they reside in groups of galaxies which significantly ionize their surroundings, allowing the Lyα photons to escape out of resonance before encountering neutral hydrogen in the IGM Wyithe & Loeb (2005); Furlanetto et al. (2006).

4.3. Comparison of LAEs and LBGs

Recent observations at $z \simeq 5$ suggest that LAEs may differ from LBGs in their typical stellar mass and ages. Observations presented in Eyles et al. (2006) have shown that $z \simeq 6$ LBGs are a composite population of galaxies, some with low stellar masses ($\simeq 10^8$ M$_\odot$) and some with high stellar masses ($\simeq 10^{10}$ M$_\odot$). These stellar masses emerge from our model given the best-fit star formation efficiency and halo masses probed by the observations. While the uncertainties are still significant, there appears to be a weak correlation between the stellar mass and age of $z \simeq 6$ LBGs (Eyles et al. 2006); the most massive galaxies appear to have a significant population of old stars (ages up to $\simeq 700$Myr), while the less massive objects appear to be much younger (ages of $\simeq 60$Myr). The model considered in this paper fixes the star formation duty cycle to be constant with halo mass and hence cannot confirm this observational inference. The best-fitting duty cycle for LBGs suggests an age of 80 Myr, which is at the low-end of the range of lifetimes expected of the LBGs.

LAEs at $z \simeq 5$ also appear to be a composite population spanning a range of masses and ages, but it appears that their typical ages and stellar masses are systematically lower than LBGs. A correlation exists between the equivalent width (EW) of the Lyα line and the galaxy age and stellar mass (Finkelstein et al. 2006). The highest EW lines exhibit the lowest ages (few million years) and stellar masses ($10^6 - 10^7$ M$_\odot$); these objects are very faint continuum emitters and hence are not selected in LBG surveys (Finkelstein et al. 2006; Pirzkal et al. 2006). LAEs with lower EWs have larger inferred ages (40-200 Myr) with stellar masses up to $\simeq 10^9$M$_\odot$ (Finkelstein et al. 2006); however, these ages and masses do not reach the values as large as those seen in LBG surveys at these redshifts. Finally, the SEDs of the young LAEs at $z \simeq 5$ suggest that there is little exinction from dust in these galaxies (Pirzkal et al. 2006). As explained in the §4.2, in order for our model to fit the observations described above, the star formation efficiency of the high EW LAEs must be low (due to their extreme youth) and transmission of Lyα photons through the host galaxy and IGM must be very high.

It is intriguing to consider the fate of the high EW LAEs. In one possible scenario, star formation continues, depleting the gas content and increasing the total stellar mass of the galaxy. The dust content of the galaxy begins to increase. The dust absorbs the resonantly-scattered Lyα photons, although the Lyα EW might be enhanced depending on geometric details (Neufeld 1991; Hansen & Oh 2006), If the star formation rate remains high, these objects could continue to be observed as LBGs. As more of the gas is converted to stars, the star formation efficiency will increase. Within our model we indeed in-

ferred that the average star formation efficiencies of the $z \simeq 6$ LBGs is on order 10%.

Alternatively, the high EW LAEs could eject their gas via feedback from supernovae explosions or quasar activity. As soon as the gas density is significantly diluted, the recombination rate decreases and there is little emission of Lyα photons. The galaxies would continue to be selected as LBGs as long as massive stars remain; however, without gas star formation eventually ceases, leaving the galaxies quiescent and with a low stellar mass. Such objects would no longer be detected as either LBGs or LAEs.

5. INTERPRETATIONS OF OBSERVATIONS AT $Z \simeq 7-10$

We now use our model fits, noting the uncertainties, to make predictions for both LBGs and LAEs observed at $z > 7$. We will assume no evolution in the model parameters to determine what redshift trends are expected solely from the natural growth of dark matter halos over the era $5 < z < 10$. A modest amount of observational data is available for the $z > 7$ universe and we will address this to see if it is consistent with no evolution. Necessarily this discussion will be tentative given the considerable uncertainty about the validity of the observations. Most of the sources claimed to lie beyond $z \simeq 7$ have no convincing spectroscopic identification.

5.1. Lyman-Break Galaxies

Preliminary constraints are now available on the abundance of LBGs at $z > 7$ (Bouwens et al. 2005; Bouwens & Illingworth 2006; Richard et al. 2006). LBGs selected as z-band dropouts are considered to be at an effective redshift $z \simeq 7.4$. The most recent compilation from fields with deep HST-NICMOS data (e.g. GOODS, UDF, UDF-P) includes one candidate in the most conservative selection and 4 candidates in a more aggressive selection (Bouwens & Illingworth 2006). After comparing the observed abundance of candidate $z \simeq 7.4$ LBGs to those at $z \simeq 6$, Bouwens & Illingworth (2006) suggest that there is a rapid assembly of the most luminous star forming systems between $z \simeq 6$ and $z \simeq 7.4$.

By extrapolating our star-formation model to $z \simeq 7.4$ and holding the parameters fixed at their best-fit $z \simeq 6$ values, we can determine whether the claimed rapid assembly of luminous galaxies requires evolution in the star formation efficiency or duty cycle. If all four candidate z-dropouts identified in Bouwens & Illingworth (2006) are at $z \simeq 7.4$, then the observed evolution in the abundance of luminous galaxies can be explained simply by evolution of the host dark matter haloes (Figure 4). However, if only one of the candidate z-dropouts is at $z \simeq 7.4$, then our simple model does permit some evolution in either the star formation efficiency or duty cycle in the 200 million years between $z \simeq 7.4$ and $z \simeq 6$. Such evolution could be triggered, for example, by the photoionization heating of the intergalactic medium at the end of reionization and the corresponding change in its accretion rate onto galaxies.

At $z \simeq 10$, several candidate LBGs (selected as J-band dropouts) have been identified in the UDF (Bouwens et al. 2005) and in cluster lensing fields (Richard et al. 2006). With the addition of deeper optical data, two of the three candidate $z \simeq 10$ LBGs from Bouwens et al. (2005) are now known to be at lower-redshift (R.J. Bouwens 2006, private communication). In this case, the abundance implied if the remaining one candidate is at $z \simeq 10$ is consistent with hierarchical growth (Figure 9). However, the abundance of less luminous
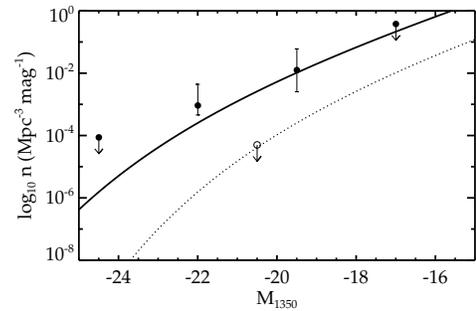

FIG. 9.— Comparison of model $z = 9$ LBG luminosity function with constraints from observations. The observed abundance of LBGs presented in the cluster lensing survey of Richard et al. (2006), denoted by solid circles, is significantly greater than the upper limit found in the Hubble Ultra Deep Field (open circle), as presented in Bouwens et al. (2006). The luminosity function obtained by assuming the duty cycle and star formation efficiency remain constant between $z = 6$ and $z = 9$ (dotted line) is unable to account for the large abundances observed in Richard et al. (2006). Reconciling these data points with our models without resorting to more top-heavy IMFs require a star formation efficiency near 100% (solid line).

$z \simeq 10$ candidates located by lensing in Richard et al. (2006) is significantly larger than expected (Figure 9). Without resorting to a more top-heavy IMF, the observed abundance of candidate $z \simeq 10$ LBGs in Richard et al. (2006) requires significant evolution in the parameters of the simple model we have adopted. Holding the duty cycle fixed at its $z \simeq 6$ value, an implausible star formation efficiency of 100% is required to explain the observed abundance (Figure 9).

The emerging physical picture describing the evolution of LBGs at $z \simeq 7\text{-}10$ is still somewhat tentative. Nonetheless, results from the UDF suggest that evolution in the abundance of *luminous* LBGs in the 500 Myr between $z \simeq 6\text{-}10$ can be largely explained by the hierarchical assembly, i.e. without any evolution in the star formation efficiency or duty cycle. In contrast, the high abundance of *less luminous* $z \simeq 10$ candidates suggested by Richard et al. (2006) can only be explained using our simple model if there is significant evolution in either the stellar IMF or the star formation efficiency. Future surveys with new facilities are required to reconcile these differing pictures. In §6, we will use our model to predict the ability of future surveys to detect starburst galaxies at $z \simeq 7\text{-}10$.

5.2. Lyα Emitters

The first results are also now available from Lyα surveys at $z \simeq 9$. As with the LBGs, the high redshift results are contradictory. Willis et al. (2005) and Cuby et al. (2006) find no Lyα emitters in narrowband surveys centered at $z = 8.8$ with the Very Large Telescope (VLT). However, both surveys are only sensitive to the brightest LAEs ($> 3 \times 10^{42}$ erg s^{-1} in Willis & Courbin 2005 and $> 10^{43}$ erg s^{-1} in Cuby et al. 2006) over modest comoving volumes (870 Mpc^3 and 5000 Mpc^3, respectively).

Stark et al. (2007) conducted a cluster lensing survey for LAEs at $z = 8.5 - 10.4$. The magnification provided by the clusters allows significantly less luminous LAEs to be detected ($\gtrsim 10^{41}$ erg s^{-1}), albeit over a much smaller comoving volume ($\simeq 30$ Mpc^3). Six candidate LAEs were identified with unlensed luminosities spanning $2\text{-}50 \times 10^{41}$ erg s^{-1}; at least two of the six candidates are considered likely to be at $z \simeq 9$ following additional spectroscopy which casts doubt on alternative low-redshift explanations for the J-band emission
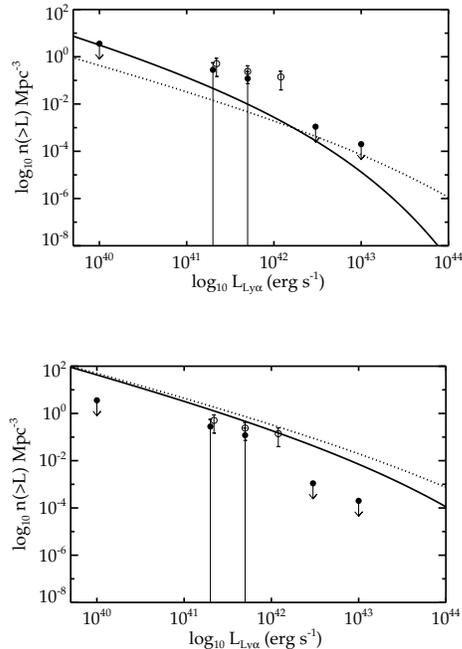
FIG. 10.— Comparison of model $z = 9$ LAE luminosity function with constraints from observations. *Top:* If all the $z \simeq 9$ LAE candidates in Stark et al. (2007) are real, then the best-fit model parameters at $z = 5.7$ (dotted line) and $z = 6.5$ (solid line) are inconsistent with their values at $z = 9$. *Bottom:* Model luminosity functions assuming an extreme top-heavy IMF characteristic of Pop-III stars with model parameters fixed at their $z = 6.5$ (dotted line) and a star formation efficiency of 100% (with duty cycle of 0.1, solid line) overlaid upon observational constraints.

features.

In Figure 10, we use our model to compute luminosity functions of LAEs at $z \simeq 9$ assuming the duty cycle, star formation efficiency, and Lyα escape fraction remain fixed at either their best-fit $z = 5.7$ or $z = 6.5$ values. As the narrowband observations refer to a single redshift, we use the mass function at $z = 8.8$ to compute the luminosity function. For the cluster lensing survey presented by Stark et al. (2007), as the halo mass function evolves significantly over the redshift range sampled, we compute the average halo mass function between $z = 8.5$ and $z = 10.4$, weighting mass by the relevant sensitivity function. The luminosity functions obtained using both mass functions are overlaid on the data points from the three surveys described above.

The results suggest that, for *luminous* LAEs, current surveys do not yet have the combined sensitivity and depth to detect any sources at $z \simeq 9$. Although the upper limits presented in Willis & Courbin (2005) and Cuby et al. (2006) are consistent with our expectations, those surveys do not usefully constrain the parameter space. On the other hand, for *less luminous LAEs*, if all six of the candidates in Stark et al. (2007) are at high- redshift, significant evolution is implied in the model parameters. As with the LBGs at $z \simeq 9$, either a high ($\simeq 100\%$) star formation efficiency (for a fixed duty cycle) or a top-heavy IMF of stars (Figure 10) would be required. However, more clusters must be observed to ensure the high observed density is not a result of large clustering fluctuations expected for such surveys. If, only the two prime LAE candidates are at high redshift[3], the derived abundances

---

[3] The fact that the Poisson errors are 100% for the two datapoints in Figure 10 corresponding to the case that two candidates from Stark et al. (2007) are

are formally consistent with the predicted $z \simeq 9$ luminosity function.

6. IMPLICATIONS FOR FUTURE SURVEYS

Over the next few years, several new instruments will be placed on current ground-based telescopes and Hubble Space Telescope motivated in part by extending the search for $z > 7$ sources. These surveys offer the exciting possibility of characterizing the assembly of the first galactic sources through the era of reionization. With our model, calibrated by the data available at $z \simeq 6$, we can consider the optimal volume and depth necessary for detecting star-forming sources of various luminosities to $z \simeq 10 - 20$. Thus it is hoped our model can assist in guiding the design of future instruments and surveys.

In the following subsections, we will evaluate several benchmark imaging and spectroscopic surveys. We consider a large, blank-field, narrowband survey for LAEs at $z \simeq 8$ and $z \simeq 10$ in §6.1, and discuss two different surveys for dropouts at $z \simeq 7.5$ and $z \simeq 10$ in §6.2. Finally, in §6.3, we examine the efficiency of a variety of lensing surveys for LAEs and LBGs. Since some of these proposed surveys reach to significantly lower luminosities than the current surveys discussed in §4 and §5, we examine the effects of feedback on the predicted counts, as well as the gains of adaptive optics given our predicted sizes for faint LAEs.

6.1. *The Dark Ages z Lyman-alpha Exlorer: LAEs at* $z \simeq 7 - 10$

The Dark Ages z Lyman-alpha Explorer (DAzLE) is a narrowband imager on the VLT which aims to detect Lyα emitters at $6.5 < z < 12$ (Horton et al. 2004). DAzLE has recently observed two pointings of GOODS-South in two filters corresponding to Lyα redshfits of $\simeq 7.7$ and $\simeq 8.0$ (R. McMahon 2006, private communication). The observing sequence for DAzLE involves alternating between two narrowband filters with slightly different central wavelengths. A composite image is made of all of the subexposures in each filter, resulting in two "subsurveys" slightly offset in redshift space. Subtracting the two composite images removes continuum soures, thereby allowing candidate LAEs to be identified.

In ten hours of integration, DAzLE is expected to reach a 3σ sensitivity of 2×10^{-18} erg cm^{-2} s^{-1} in the differenced image (Horton et al. 2004). At $z = 7.7$, this corresponds to a limiting LAE luminosity of 1.5×10^{42} erg s^{-1}. As a benchmark survey with this instrument, we consider a four position mosaic (i.e. $4 \times 6.'83 \times 6.'83$). The total comoving volume sampled in four pointings of the two filters at $z = 7.7$ is $\simeq 7200$ Mpc^3. A simple extrapolation of our model suggests that a comoving volume of 1100-1300 Mpc^3 is necessary to detect one LAE at $z = 7.7$. Thus, in this proposed survey, 6-7 LAEs would be detected with DAzLE assuming no rapid evolution in the star formation efficiency, duty cycle or IGM transmission between $z \simeq 6.5$ and $z \simeq 7.7$.

However, although a promising survey in terms of likely detections, the uncertainties are considerable. Clustering fluctuations are 40-50% (for the best-fit z=5.7 and 6.5 model parameters, respectively) at the limiting luminosity of 1.5×10^{42} erg s^{-1}. The expected Poisson fluctuations are similar - $\simeq 43\%$. It is prudent to consider what effects such large

real may seem counterintuitive given that there are two sources; however this arises from strongly-varying limiting (detectable) source luminosity over the field of view due to the cluster magnification. For details, see Stark et al. (2007).
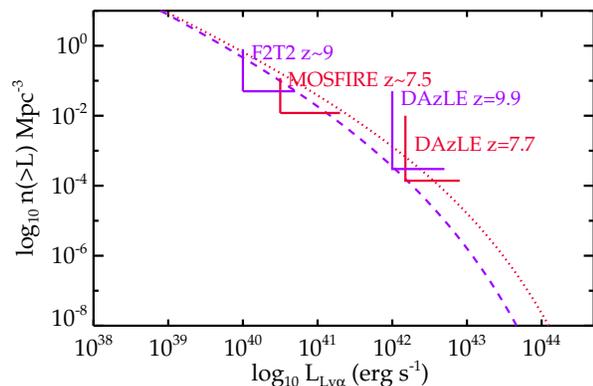
FIG. 11.— Extrapolation of Lyα luminosity function to $z \simeq 7.7$ (dotted red curve) and 10 (dashed purple curve) fixing star formation model parameters at their best-fit $z = 6.5$ values (§4). The predicted luminosity function suggests that DAzLE should detect 6-7 $z \simeq 7.7$ sources in a four pointing mosaic with total integration time of $\simeq 40$ hours. Over 200 hours are required to detect a single $z \simeq 10$ source under these assumptions. The estimated performance of lensing surveys with a multi-object spectrograph such as MOSFIRE or a tunable narrowband filter (F2T2) suggest that lensing is an efficient means of detecting LAEs at $z \simeq 7-10$, but supernova feedback could drastically reduce the number of LAEs detected.

fluctuations would have on attempts at using the DAzLE results to constrain the progress of reionization via the evolution of the LAE luminosity function (Malhotra & Rhoads 2004, 2006; Dijkstra et al. 2006). While our model predicts that 6-7 sources should be detected assuming only evolution in the underlying halos, the large ($\simeq 60\%$) expected fluctuations imply that the source counts could vary significantly from the predicted value. Ignoring additional complications on the tranmission of Lyα photons through the IGM from galaxy groups (Wyithe & Loeb 2005; Furlanetto et al. 2004, 2006) and peculiar velocities (Dijkstra & Loeb 2006, in preparation), if between two and ten LAEs are detected with DAzLE in GOODS-S, little information can be reliably deduced on the evolution of IGM. Holding the duty cycle and star formation efficiency fixed, it would require a $\gtrsim 60\%$ decrease in the Lyα transmission factor, T_α, for only one $z = 7.7$ LAE to be detected towards GOODS-S. Hence, these results suggest that, with currently feasible survey geometries and instruments, this method of constraining reionization will only be effective if the IGM evolves rapidly ($\gtrsim 60\%$) over a short redshift interval.

DAzLE is also designed to search for LAEs out to $z \simeq 10$. There is a large gap in the atmospheric OH forest between 1.3325 μm and 1.3401 μm, corresponding to a LAE redshift window of $\Delta z = 0.006$ centered at $z = 9.99$. A similar window is located at $z = 9.91$. A single DAzLE pointing at this redshift samples a comoving volume of $\simeq 1000 \text{Mpc}^3$ summed over both filters. Extrapolating the model luminosity function to this redshift with the parameters fixed at their best-fit $z = 6.5$ values, it would take just over a volume of 3000 Mpc^3 (three pointings) to detect one LAE brighter than 10^{42} erg s^{-1}. At $z = 9.99$, this luminosity limit corresponds to a limiting flux of 8×10^{-19} erg cm^{-2} s^{-1}. Reaching this sensitivity would require 70–80 hours for each pointing (adjusting for the expected atmospheric transparancy in the wavelength interval of the observations); hence over 200 hours would be required to detect a single $z \simeq 10$ source. Alternatively, if the LAE candidates identified by Stark et al. (2007) are at high-redshift, then

140 LAEs brighter than 10^{42} erg s^{-1} would be expected in the single 70-80 hour DAzLE pointing.

In summary, DAzLE may well detect many z=7.7 sources but spectroscopic confirmation will be a challenge. However, even in the most ambitious surveys we can currently contemplate, the contribution of these sources to reionization will be seriously limited by the expected clustering fluctuations. Surveys at higher redshift will be much more demanding. Few sources are expected within reasonable exposure times at $z \simeq 9$–10 unless there is significant evolution in the LAE model parameters between $6 < z < 10$, as may be possible only if all of the fainter lensed LAEs detected by Stark et al. (2007) are at high redshift.

6.2. Imaging Surveys for LBGs at $z \simeq 7 - 10$

Selection of $z \gtrsim 7$ LBGs will be greatly aided by the new generation of large-format near-infrared detectors. The Subaru Multi-Object Infrared Camera and Spectrograph (MOIRCS, Ichikawa et al. 2006) offers imaging and spectroscopic capabilities over a large $4' \times 7'$ field of view. In 2008, WFC3 is scheduled to be installed on HST; this near-IR camera will offer imaging in a $127.0'' \times 137.0''$ field of view. We thus consider likely surveys with MOIRCS and WFC3. First we consider a MOIRCS wide-field mosaic whose sensitivity is arranged to match that of the near-infrared observations of GOODS-S, but with an area twice as large. We then consider a single, ultra-deep pointing with WFC3.

To observe an area twice as large of GOODS-S would require eleven MOIRCS pointings. Selecting reliable z-dropouts ($z \simeq 7.5$) and J-dropouts ($z \simeq 10$) requires deep z, J, H, and K-band data. We assume the near-infrared data is roughly similar in depth to GOODS, with 5-σ point sources sensitivies of z'=26.6, J=25.8, H=24, and K=24. These limits are optimized to the selection criteria of z'-drops (z'-J>0.8, Bouwens & Illingworth 2006) and J-drops (J-H>1.8, Bouwens et al. 2005). The K-band limit is chosen with the goal of detecting J-drops in a second filter to help remove false-positives. The limiting J- and H-band limits correpond to limiting star formation rates of 18 and 146 M$_\odot$yr^{-1} at $z \simeq$ 7.5 and 10, respectively. Reaching J=25.8 with MOIRCS requires $\simeq 12$ hours of integration assuming 0.''5 seeing (J. Richard 2006, private communication). Significantly less time is needed to reach the desired sensitivies in H (1.8 hours) and K (40 minutes). The z'-band observations would be most efficiently performed with the Suprime-Cam on Subaru. The entire area could be covered in one pointing with Suprime-Cam, requiring 4.7 hours of integration. In total, 163 hours would be required for the observing sequence. We consider this a practical, albeit ambitious, program.

Each MOIRCS field of view samples a comoving area of 10.6 Mpc × 18.6 Mpc at $z \simeq 7.5$ and 11.9 Mpc × 20.9 Mpc at $z \simeq 10$. Following simulations conducted in Bouwens et al. (2005) and Bouwens & Illingworth (2006), we assume the redshift probability distribution of z-drops and J-drops is a Gaussian with a standard deviation of σ_z=0.5 and a mean of μ_z=7.5 and 10 for z-drops and J-drops, respectively. Over eleven pointings, this corresponds to a total comoving volume of 1.5×10^5 Mpc^3 at $z \simeq 7.5$ and 1.0×10^5 Mpc^3 at $z \simeq 10$.

In Figures 12 and 13, we extrapolate the best-fit luminosity function from $z \simeq 6$ to $z \simeq 7.5$ and $z \simeq 10$ allowing only for evolution in the dark matter mass function. The comoving number density of detected LBGs is 8.2×10^{-6} Mpc^{-3} mag^{-1} at $z \simeq 7.5$ and 1.1×10^{10} Mpc^{-3} mag^{-1} at $z \simeq 10$. Integrating over the entire magnitude range, 0.5 sources would be
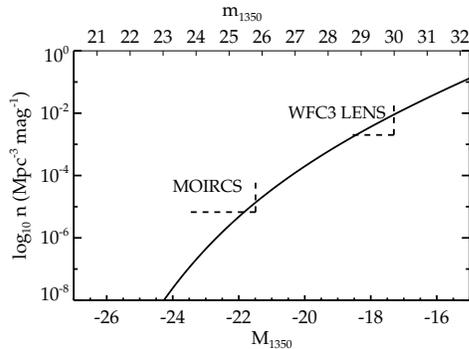
FIG. 12.— Predicted LBG luminosity function at $z \simeq 7.5$ assuming star formation model parameters are fixed at their best-fit $z \simeq 6$ values (§4). The absolute magnitude at 1350Å is plotted horizontally along the bottom of the plot, and the corresponding J-band apparent magnitude is plotted along the top of the plot, assuming $z = 7.5$. The efficiency of several mock surveys for $z \simeq 7.5$ sources is overplotted.
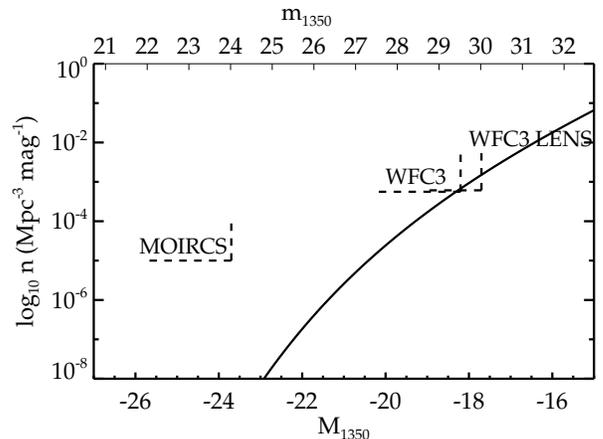

FIG. 13.— Predicted LBG luminosity function at $z \simeq 10$ assuming star formation model parameters are fixed at their best-fit $z \simeq 6$ values (§4). The absolute magnitude at 1350 Å is plotted horizontally along the bottom of the plot, and the corresponding H-band apparent magnitude is plotted along the top of the plot, assuming $z = 10$. The efficiency of several mock surveys for $z \simeq 10$ sources is overplotted.

detected brighter than J=25.8 at $z \simeq 7.5$ and 2×10^{-6} sources would be detected brighter than H=24 at $z \simeq 10$, where the number in paranthesis corresponds to the equivalent number detected when supernova feedback is accounted for. Clearly, neither the $z \simeq 7.5$ or $z \simeq 10$ MOIRCS mock-survey is very efficient at detecting high-redshift sources. Even with the relatively large areal coverage provided by MOIRCS, the integrated near-infrared sky is simply too bright in broadband filters to reach the sensitivity limits necessary to detect an abundant population of $z \gtrsim 7-10$ LBGs; with current technology, ground-based surveys are much better off searching for LAEs using narrower filters tuned in between the bright sky lines.

As with the MOIRCS observations, the mock WFC3 observations require deep z, J, and H-band coverage to select z- and J-band dropouts. WFC3 offers a significant improvement in both throughput and areal coverage with respect to NICMOS, so the camera is ideal for selecting J-drops in a single pointing. By contrast, WFC3 is *not* more efficient than ACS in the z-band. Therefore, WFC3 is not particularly well-suited for conducting a new z-drop survey that is significantly deeper than UDF. We thus imagine its principal goal will be the detection of J-dropouts.

We adopt limiting magnitudes that are $\simeq 1$ and $\simeq 2$ magnitudes deeper than the UDF in H_{160} and J_{110}, respectively, corresponding to 5σ sensitivities of $J_{110}=30.6$ and $H_{160}=29.5$ for point sources. The estimated star formation rate for $z \simeq 10$ LBGs with $H_{160}=29.5$ is $0.9\,\mathrm{M}_{\odot}yr^{-1}$. Based on the anticipated WFC3 performance, reaching such sensitivities in a single pointing would take 275 hours in J_{110} and 158 hours in H_{160W} resulting in 433 hours of total integration [4]. Since K-band observations are not practical with WFC3, we rely only on an H-band detection for J-drop selection. Each WFC3 field of view covers a comoving area of $6.0\,\mathrm{Mpc} \times 6.5\,\mathrm{Mpc}$ at $z \simeq 10$. Assuming a redshift probability distribution identical to that described above for z-drops and J-drops with MOIRCS, we find that the single WFC3 pointing will sample a comoving volume of $1800\,\mathrm{Mpc}^3$ at $z \simeq 10$.

The predicted comoving number density of detected J-drop LBGs in the single deep WFC3 pointing is $4.9 \times 10^{-4}\,\mathrm{Mpc}^{-3}\,\mathrm{mag}^{-1}$ at $z \simeq 10$, assuming no-evolution in the star formation efficiency and duty cycle. Integrating over the en-

tire magnitude range, 0.5 sources would be detected at $z \simeq 10$.

In summary, existing ground-based imagers are not well-equipped for detecting LBGs at $z \simeq 7-10$, largely because the integrated near-IR sky is too bright to reach the sensitivity limits necessary to detect sources at $z \gtrsim 7$ in a reasonable amount of time. This problem could be lessened if the field of view was much bigger, allowing the the most luminous and rare LBGs to be detected. Even from space (using WFC3 on HST), detecting LBGs at $z \simeq 7-10$ will not be trivial, requiring hundreds of hours to detect a single LBG at $z \simeq 10$.

6.3. *Lensing Surveys for Star-forming Galaxies at $z \simeq 7-10$*

Currently, strong lensing surveys for high-redshift galaxies could be contemplated for about 20 galaxy clusters for which there are well-defined mass models; these mass models are essential in accurately defining the spatial distribution of magnification. However, ongoing HST surveys will significantly increase the number of suitable galaxy clusters (e.g. Ebeling et al. 2003). Here, we examine the efficiency of surveys for lensed LBGs and LAEs assuming a larger sample of clusters and more efficient instruments that will soon become available. We consider both an extension of the longslit spectroscopic survey discussed in (Stark et al. 2007) and as well as an imaging campaign to identify lensed z-drops and J-drops.

In the next several years, a number of near-IR multi-object spectrometers will be installed on 8-10 meter class telescopes, offering significant gains in sensitivity and field-of-view over current near-IR instruments. One such instrument is the Multi-Object Spectrograph For Infra-Red Exploration (MOS-FIRE, PI: I. McLean & C. Steidel) on Keck I. MOSFIRE will utilize a configurable slit unit allowing up to 45 slits, each 7″3 in length, within the 6.′14×6.′14 field of view. While tilted and curved slits are not possible with MOIRCS, the configurable slit unit will still allow for more areal coverage of high magnification regions than with NIRSPEC. In addition, MOS-FIRE will be more sensitive than NIRSPEC, reaching 5σ line flux sensitivities of $1 \times 10^{-18}\,\mathrm{erg\,cm^{-2}\,s^{-1}}$ in 4 hours, assuming an unresolved line with R=3270 [5]. Given the specifications of

---

[4]   Estimated   sensitivies   for   WFC3   are   listed   at http://www.stsci.edu/hst/wfc3/documents/handbook/ cycle16/wfc3_cyc166.html

[5]   Sensitivities   and   additional   specifications   of   the   spectrograph   are   provided   in   the   Preliminary   Design   Report

MOSFIRE, it is optimal to concentrate observations to clusters with vary large and well-determined critical lines (e.g. Abell 1689, Abell 1703, Abell 2218). While the exact magnification distribution provided to background sources may very slightly from cluster to cluster, it is reasonable to expect 80% of the MOSFIRE survey area to be at a magnification of 20, 15% of the area to have a magnification of 10, and 5% of the area to be magnified by only a factor of 5 (Stark et al. 2007).

We consider a MOSFIRE *spectroscopic* lensing survey for LAEs both at $z = 7.0 - 8.3$ (Y-band) and at $z = 8.5 - 10.3$ (J-band). Assuming $\simeq 15\%$ of the line-of-sight distance is lost due to bright OH lines, this corresponds to comoving radial distances of 353 and 334 Mpc, respectively. Assuming 10 clusters are observed for 8 hours each in the Y-band, the resulting survey volume is $\simeq 83\,\mathrm{Mpc}^3$ for LAEs brighter than $10^{40.5}\mathrm{ergs}^{-1}$. For the mock J-band survey, we assume longer integration times (20 hours) and fewer clusters (5). This results in the coverage of $\simeq 52\,\mathrm{Mpc}^3$ for $z \simeq 10$ LAEs brighter than $10^{40.5}\mathrm{ergs}^{-1}$. Extrapolating our LAE model to $z = 7.5$ and to $z = 10$ holding the model parameters fixed at their $z = 5.7$ values, we predict that the MOSFIRE survey should detect $\simeq 10$ sources brighter than $10^{40.5}\mathrm{ergs}^{-1}$ at $z = 7.5$ and 3 sources brighter than this limit at $z \simeq 10$. If supernova feedback decreases the star formation efficiency in a manner described in §2, then the predicted number of LAEs would drop drastically. The $z \simeq 7.5$ survey would potentially detect 1 LAE brighter than $10^{40.5}\mathrm{ergs}^{-1}$ while the $z \simeq 10$ survey would not detect any sources. Hence, the success of the mock lensing survey depends strongly on whether supernova feedback decreases the efficiency of star formation in low-mass dark matter halos. Given the possible efficiency with which the lensing survey could detect $z \simeq 7-10$ galaxies, it is of the utmost importance to observationally constrain the effects of supernova feedback on the LAE luminosity function at lower redshifts ($z \simeq 3-6$).

Gravitational lensing can also be very valuable for *imaging* surveys for LBGs that are intrinsically fainter than those detected in conventional deep surveys (e.g. GOODS, UDF). One such survey is currently being conducted toward six galaxy clusters with NICMOS on HST (Stark & Ellis 2006, Richard et al. 2007, in preparation). With WFC3, such a survey could potentially be conducted much more efficiently, allowing many more clusters to be observed. We examine the feasibility of a hypothetical WFC3 lensing survey of galaxy clusters for z- and J-dropout galaxies.

The primary benefit of a WFC3 survey for $z \gtrsim 7$ LBGs is the added throughput and field of view in the J_{110} and H_{160}-bands compared to what is available with NICMOS. For each cluster, we assume 5-σ point-source sensitivities (in an aperture with $0.''4$ diameter) of $z_{850}=27.8$, $J_{110}=28.2$, and $H_{160}=27.4$, requiring 7, 1, and 1 hour(s) per cluster, respectively [6]. These limits allows z-drops to be selected down to J=26 and H=27.4 (without considering the effects of lensing). If we allot 180 hours to this observing program (corresponding to less integration time than the UDF), 20 clusters can be observed. The total area surveyed is more than a factor of three greater than previous lensing surveys for $z \gtrsim 7.5$ LBGs (Richard et al. 2006, in preparation).

Both the survey volume and limiting source luminosity are modified by the magnification provided by the foreground galaxy cluster (see Santos et al. 2004 or Stark et al. 2007 for a description). A typical cluster provides a magnification boost of $\times 2, 5, 10$, and 30 over 86%, 39%, 25%, and 11% of the entire WFC3 field of view. Adopting this magnification distribution for each of the 20 clusters, at $z \simeq 7.5$, the survey is sensitive to a volume of 2.2^5, 6.1×0^4, 1.2×10^4, 2600, and 510 Mpc³ for sources brighter than $J_{110} = 26, 27, 28, 29$, and 30 respectively. At $z \simeq 10$, the survey probes a comoving volume of 1.1×10^5, 2.8×10^4, 5500, 1200, and 240 Mpc³ for sources brighter than $H_{160}=27.4, 28.4, 29.4$, and 30.4, respectively. Over 20 clusters, if the star formation efficiency and duty cycle remain fixed, then such a survey should detect 18 $z \simeq 7.5$ LBGs brighter than J=30 (corresponding to a star formation rate of 0.4 $M_\odot \mathrm{yr}^{-1}$ for the source assumptions discussed in §2, Figure 12) and 4 $z \simeq 10$ LBGs brighter than H=30 (corresponding to a star formation rate of 0.6 $M_\odot \mathrm{yr}^{-1}$, Figure 13).

Adaptive optics (AO) provides the possibility of diffraction-limited observations from the ground. If the projected size of the target objects is small enough, such observations are more efficient than non-AO observations because the photometric aperture can be decreased, thereby allowing significantly less noise for nearly the same amount of flux[7]. One planned survey that aims to take advantage of AO is the Gemini Genesis Survey (GGS). This survey will use a tunable Fabry-Perot etalon (F2T2, Scott et al. 2006) on Gemini with resolution of R=800 to detect lensed LAEs at $z \simeq 8-10$. If the projected angular size of the sources is less than $\simeq 0.03$ arcsec², then GGS should be able to reach a 5σ sensitivity of $6 \times 10^{-18}\mathrm{ergcm}^{-2}\mathrm{s}^{-1}$ in 10 minutes (R. Abraham 2006, personal communication). Following the scaling relation derived in §2, galaxies at $z \simeq 10$ should have typical sizes of 0.01 arcsec², small enough to significantly benefit from AO. The field of view of F2T2 is $45.''\times45.''$, ideally suited to imaging the most highly magnified regions of galaxy clusters. We conside a mock GGS survey of 20 clusters; we assume each cluster is observed for 10 minutes in 40 different wavelength positions between 1.1μm and 1.3μm, allowing the detection of LAEs at $z = 8.1$ to $z = 9.7$. Allowing for overheads, this should take $\simeq 150$ hours of integration. A typical cluster provides a magnification gain of $\times 5, 10,$ and 30 over $80\%, 69\%$, and 33% of the F2T2 field of view. Taking this as the magnification distribution for each of the clusters, the total survey volume sensitive to LAEs brighter than $10^{40}\mathrm{ergs}^{-1}$ is 20 Mpc³. The $z \simeq 9$ LAE luminosity function (assuming fixed model parameters from $z = 5.7$) suggests that 5–6 sources would be detected at $z \simeq 9$. If the effects of supernova feedback are parameterized as in §2 and §4, the number density of low luminosity sources is drastically reduced; in this case, no sources would be detected in the survey.

It appears that lensing surveys offer one of the more efficient means of identifying galaxies at $z \simeq 7-10$ since they are able to reach sensitivity limits where objects are expected to be much more abundant. However, supernova feedback may drastically reduce the number of sources detected in these surveys. Regardless, spectroscopic confirmation of these sources will continue to remain challenging until JWST and 20-30 meter ground-based telescopes become available.

---

located at http://www.astro.ucla.edu~irlab/mosfire/MOSFIRE%20PDR%20Report%20v4.pdf

[6] ACS sensitivities are determined with the exposure time calculator available at http://apt.stsci.edu/webetc/acs/acs_img_etc.jsp

[7] The validity of this statement depends on the strehl ratio, which is the ratio of the peak brightness of the stellar image to that produced by an ideal optical system. If the strehl is very low, then the amount of flux in the diffraction-limited aperture will be greatly reduced.

7. CONCLUSIONS

We have attempted to empirically calibrate the parameters of a simple star formation model using observations of star-forming galaxies (both LBGs and LAEs) at $z \simeq 6$. The error budget used in fitting the data takes proper account of both the Poisson and clustering variance. We use the calibrated model to characterize the physical properties of LBGs and LAEs at $z \simeq 6$ and extrapolate it to higher redshifts to make predictions for upcoming surveys for galaxies at $z \simeq 7 - 10$. Our primary conclusions are as follows:

1. We have derived accurate formulae for the field-to-field variance expected in broadband surveys for LBGs, narrow-band surveys for LAEs, and lensing surveys for LAEs. For each survey geometry, there exists a cross-over luminosity L_c below which the clustering variance dominates over commonly-used Poisson variance. In total, the clustering variance accounts for less than 6% error in narrowband surveys for LAEs in the Subaru Deep Field and less than 19% error in the $z \simeq 6$ surveys for LBGs in UDF. The clustering fluctuations are significantly higher for spectroscopic lensing surveys reaching up to 100%.

2. LBGs at $z \simeq 6$ are best-fit by a model with a star formation efficiency of 10% and a duty cycle of 0.08. The star formation efficiency suggests that 90% of the baryonic mass of $z \simeq 6$ LBGs still remains in the gas-phase. The duty cycle indicates that the current burst of star formation has a lifetime of 80 Myr, roughly equivalent to the dynamical time of virialized halos at $z \simeq 6$. The duty cycle also implies that 92% of dark matter halos of a given mass are not traced by LBGs. The missing halos could have yet to form many stars (due perhaps to inefficient cooling) or could be quiescent after experiencing a burst of star formation at earlier times. This result suggests that the claimed deficit in ionizing photons from luminous LBGs at $z \simeq 6$ relative to what is required for reionization may be explained by star formation at higher redshift.

3. The best-fitting model parameters for LAEs show some evidence for evolution between $z = 5.7$ and $z = 6.5$. However, most likely the evolution is not due to a change in the neutral fraction of the IGM since the parameter that is proportional to the transmission of Lyα photons through the IGM *increases* between $z = 5.7$ and $z = 6.5$. Thus, we consider the evolution to be tentative because of the large uncertainties in the density of the lowest luminosity LAEs. Additional spectroscopic efforts are needed to improve the spectroscopic completeness at low-luminosities.

4. The star formation efficiency of LAEs must be very low ($\simeq 1\%$) in order to reproduce the low stellar masses inferred from observations of LAEs at $z \simeq 5$. Such a low star formation efficiency is only possible in the context of the models if the Lyα transmission factor is near unity. This not only requires a large escape fraction of Lyα photons from the galaxy, but also requires that the photons are not substantially absorbed in their path through the IGM. The emerging physical picture

is that the LAEs are young objects (10-20 Myr) that have only converted 1% of their baryons to stars (and hence remain gas-rich) and have not yet produced much dust, allowing a large escape fraction for Lyα photons. The intergalactic absorption decrement in Lyα may be reduced if the ionizing luminosity of the LAEs or the galaxy groups in which they reside is sufficiently large so as to strongly ionize the IGM in their vicinity.

5. We have attempted to fit preliminary data at $z \simeq 7 - 10$ by extrapolating our model to higher redshifts assuming model parameters are fixed at their calibrated $z \simeq 6$ values. The observed evolution of LBGs between $z \simeq 6$ and $z \simeq 7.5$ can be explained largely by changes in the host dark matter halos. At $z \simeq 10$ the picture is more complicated. Constraints on the presence of $z \simeq 10$ LBGs in the Hubble UDF (Bouwens et al. 2005) are explained by the hierarchical growth of dark matter halos. In contrast, the large abundance of $z \simeq 10$ LBGs in the lensing survey of Richard et al. (2006) is difficult to explain without resorting to a top-heavy IMF. The situation is similar for the LAEs. Two conventional surveys at $z = 8.8$ are consistent with no-evolution in the model parameters from $z = 5.7$, while the abundances inferred from candidate LAEs in a spectroscopic lensing survey (Stark et al. 2007) are only explainable if the IMF is top-heavy.

6. New instruments that will become available on ground-based telescopes and HST in the next 2-3 years should greatly increase the efficiency with which $z \simeq 7 - 8$ LAEs and LBGs are detected. However, unless there is significant upward evolution in the luminosity function from $z \simeq 6$, detecting $z \simeq 10$ galaxies via conventional methods will only be feasible if heroic efforts are undertaken. With current telescopes, lensing surveys are potentially better suited to detecting $z \simeq 10$ sources depending on supernova feedback. JWST and thirty-meter class ground-based telescopes are most likely necessary to detect a substantial population of objects at $z \simeq 10$.

7. Constraining reionization at $z \simeq 6 - 7$ via the evolution in the LAE luminosity function as probed by future narrowband surveys will be complicated by clustering and Poisson variance. Given the large fluctuations ($\gtrsim 60\%$ for feasible survey geometries and sensitivities) and small number of sources expected to be detected ($\simeq 7$ assuming no evolution from z=5.7), this technique will only be effective if the neutral fraction in the IGM evolves very rapidly in the redshift interval between $z = 6.5$ and $z = 7.7$.

REFERENCES

Babich, D., & Loeb, A. 2006, ApJ, 640, 1
Barkana, R., & Loeb, A. 2000, ApJ, 531, 613
Barkana, R., & Loeb, A. 2006, MNRAS, 371, 395
Bouwens, R. J., & Illingworth, G. D. 2006, Nature, 443, 189
Bouwens, R. J., Illingworth, G. D., Blakeslee, J. P., Broadhurst, T. J., & Franx, M. 2004, ApJ, 611, L1
Bouwens, R. J., Illingworth, G. D., Blakeslee, J. P., & Franx, M. 2006, ApJ, 653, 53
Bouwens, R. J., Illingworth, G. D., Thompson, R. I., & Franx, M. 2005, ApJ, 624, L5

Bromm, V., Kudritzki, R. P., & Loeb, A. 2001, ApJ, 552, 464
Bruzual, G., & Charlot, S. 2003, MNRAS, 344, 1000
Bunker, A. J., Stanway, E. R., Ellis, R. S., & McMahon, R. G. 2004, MNRAS, 355, 374
Cuby, J. ., Hibon, P., Lidman, C., Le Fevre, O., Gilmozzi, R., Moorwood, A., & van der Werf, P. 2006, Accepted for Publication in A&A, astro-ph/0611272
Dekel, A., & Woo, J. 2003, MNRAS, 344, 1131
Dijkstra, M., Wyithe, S., & Haiman, Z. 2006, ArXiv Astrophysics e-prints

Ebeling, H., Edge, A., Barrett, E., Donovan, D., van Speybroeck, L., Courtney, N., & Joy, M. 2003, The Cosmic Cauldron, 25th meeting of the IAU, Joint Discussion 10, 18 July 2003, Sydney, Australia, 10

Ellis, R. S. 2007, astro-ph/0701024

Eyles, L., Bunker, A., Ellis, R., Lacy, M., Stanway, E., Stark, D., & Chiu, K. 2006, Accepted for publication in MNRAS, astro-ph/0607306

Eyles, L. P., Bunker, A. J., Stanway, E. R., Lacy, M., Ellis, R. S., & Doherty, M. 2005, MNRAS, 364, 443

Fan, X., Carilli, C. L., & Keating, B. 2006, ARA&A, 44, 415

Finkelstein, S. L., Rhoads, J. E., Malhotra, S., Pirzkal, N., & Wang, J. 2006, ArXiv Astrophysics e-prints

Fukugita, M., Hogan, C. J., & Peebles, P. J. E. 1998, ApJ, 503, 518

Furlanetto, S. R., Zaldarriaga, M., & Hernquist, L. 2004, ApJ, 613, 1

Furlanetto, S. R., Zaldarriaga, M., & Hernquist, L. 2006, MNRAS, 365, 1012

Gawiser, E., et al. 2006, ApJ, 642, L13

Gnedin, N. Y., & Fan, X. 2006, ApJ, 648, 1

Hansen, M., & Oh, S. P. 2006, MNRAS, 367, 979

Horton, A., Parry, I., Bland-Hawthorn, J., Cianci, S., King, D., McMahon, R., & Medlen, S. 2004, in Ground-based Instrumentation for Astronomy. Edited by Alan F. M. Moorwood and Iye Masanori. Proceedings of the SPIE, Volume 5492, pp. 1022-1032 (2004)., ed. A. F. M. Moorwood & M. Iye, 1022

Hu, E. M., Cowie, L. L., Capak, P., McMahon, R. G., Hayashino, T., & Komiyama, Y. 2004, AJ, 127, 563

Ichikawa, T., et al. 2006, in Ground-based and Airborne Instrumentation for Astronomy. Edited by McLean, Ian S.; Iye, Masanori. Proceedings of the SPIE, Volume 6269, pp. 626916 (2006).

Iye, M., et al. 2006, Nature, 443, 186

Kaiser, N., & Peacock, J. A. 1991, ApJ, 379, 482

Kashikawa, N., et al. 2006, ApJ, 648, 7

Kayo, I., Taruya, A., & Suto, Y. 2001, ApJ, 561, 22

Le Delliou, M., Lacey, C., Baugh, C. M., Guiderdoni, B., Bacon, R., Courtois, H., Sousbie, T., & Morris, S. L. 2005, MNRAS, 357, L11

Loeb, A. 2006, ecture notes for the SAAS-Fee Winter School, April 2006 (to be published by Springer Verlag), astro-ph/0603360

Loeb, A., Barkana, R., & Hernquist, L. 2005, ApJ, 620, 553

Madau, P., Pozzetti, L., & Dickinson, M. 1998, ApJ, 498, 106

Malhotra, S., & Rhoads, J. E. 2004, ApJ, 617, L5

Malhotra, S., & Rhoads, J. E. 2006, ApJ, 647, L95

Mao, J., Lapi, A., Granato, G. L., de Zotti, G., & Danese, L. 2006, Submitted to ApJ, astro-ph/0611799

Miyazaki, S., et al. 2002, PASJ, 54, 833

Nagamine, K., Cen, R., Hernquist, L., Ostriker, J. P., & Springel, V. 2005, ApJ, 618, 23

Neufeld, D. A. 1991, ApJ, 370, L85

Overzier, R. A., Bouwens, R. J., Illingworth, G. D., & Franx, M. 2006, ApJ, 648, L5

Pirzkal, N., Malhotra, S., Rhoads, J. E., & Xu, C. 2006, ArXiv Astrophysics e-prints

Richard, J., Pelló, R., Schaerer, D., Le Borgne, J.-F., & Kneib, J.-P. 2006, A&A, 456, 861

Santos, M. R., Ellis, R. S., Kneib, J.-P., Richard, J., & Kuijken, K. 2004, ApJ, 606, 683

Schaerer, D. 2003, A&A, 397, 527

Scott, A., et al. 2006, in Ground-based and Airborne Instrumentation for Astronomy. Edited by McLean, Ian S.; Iye, Masanori. Proceedings of the SPIE, Volume 6269, pp. 62695J (2006).

Shapley, A. E., Steidel, C. C., Erb, D. K., Reddy, N. A., Adelberger, K. L., Pettini, M., Barmby, P., & Huang, J. 2005, ApJ, 626, 698

Sheth, R. K., Mo, H. J., & Tormen, G. 2001, MNRAS, 323, 1

Shimasaku, K., et al. 2006, PASJ, 58, 313

Smith, R. E., et al. 2003, MNRAS, 341, 1311

Somerville, R. S., Lee, K., Ferguson, H. C., Gardner, J. P., Moustakas, L. A., & Giavalisco, M. 2004, ApJ, 600, L171

Spergel, D. N., et al. 2006, Submitted to ApJ, astro-ph/0603449

Stark, D. P., Bunker, A. J., Ellis, R. S., Eyles, L. P., & Lacy, M. 2006, accepted for publication in ApJ, astro-ph/0604250

Stark, D. P., & Ellis, R. S. 2006, New Astronomy Review, 50, 46

Stark, D. P., Ellis, R. S., Richard, J., Kneib, J. P., Smith, G. P., & Santos, M. R. 2007, accepted for publication in ApJ, astro-ph/0701279

Willis, J. P., & Courbin, F. 2005, MNRAS, 357, 1348

Wyithe, J. S. B., & Loeb, A. 2005, ApJ, 625, 1

Wyithe, J. S. B., & Loeb, A. 2006, Nature, 441, 322

Yan, H., Dickinson, M., Giavalisco, M., Stern, D., Eisenhardt, P. R. M., & Ferguson, H. C. 2006, ApJ, 651, 24

TABLE 1
VARIANCE IN HIGH-Z GALAXY SURVEYS

Field	Type	Field of View (arcmin^2)	z	$L_{Lya,c}$ (erg s^{-1})	L_{1500} (erg s^{-1} Hz^{-1})	$\sigma^2_{F2F}(L_c)$
GOODS	dropout	160	6	N/A	$10^{28.1}$	0.003
UDF	dropout	11	6	N/A	$10^{28.3}$	0.05
SDF	narrowband	1295	5.7	$10^{41.7}$	N/A	0.001
Cluster	spec. lensing	0.13	8.5-10.4	N/A	N/A	N/A

NOTE. — The field of view for the spectroscopic lensing survey is in the source plane, assuming a median magnification of 10. The crossover luminosity is listed as "N/A" for the lensing survey because the clustering fluctuations are greater than the Poisson noise for all luminosities over which our model predicts sources should be detected.